Chemosphere 357 (2024) 141912

Contents lists available at ScienceDirect

Chemosphere

journal homepage: www.elsevier.com/locate/chemosphere

Magnetite-driven Bio-Fenton degradation of chloroacetanilide herbicides by a newly isolated hydrogen peroxide producing bacterium Desemzia sp. strain C1

Yongseok Ko [a], Sunil Ghatge [a], Hor-Gil Hur [a,**], Youri Yang [b,*]

[a] School of Earth Sciences and Environmental Engineering, Gwangju Institute of Science and Technology (GIST), Gwangju, 61005, Republic of Korea
[b] School of Natural Resources and Environmental Science, Department of Biological Environment, Kangwon National University, Chuncheon, Gangwon State, 24341, Republic of Korea

HIGHLIGHTS

- H_2O_2-producing *Desemzia* sp. strain C1 was isolated from oil-contaminated soil.
- Bio-Fenton reaction was performed using magnetite and H_2O_2 by strain C1 at pH 6.8.
- Optimal conditions for an efficient Bio-Fenton reaction were investigated.
- Chloroacetanilide herbicides were chosen as a model of environmental pollutants.
- The herbicides were degraded via non-specific oxidative reaction of .•OH.

GRAPHICAL ABSTRACT

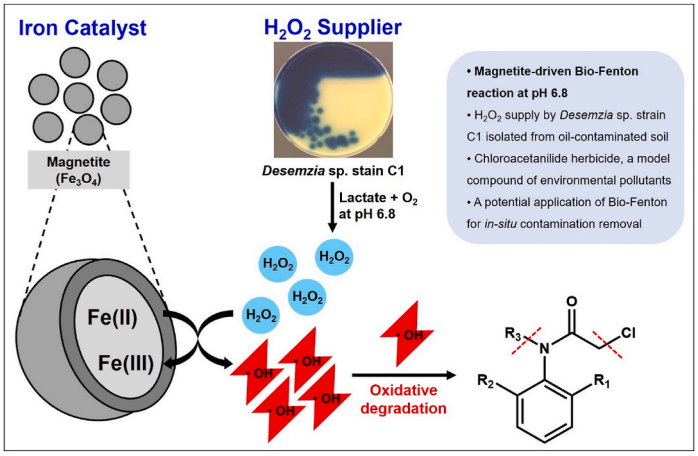

ARTICLE INFO

Handling Editor: Y Yeomin Yoon

Keywords:
Desemzia sp. strain C1
Bio-Fenton reaction
Magnetite
Hydroxyl radical
Hydrogen peroxide

ABSTRACT

The efficiency of the Fenton reaction is markedly contingent upon the operational pH related to iron solubility. Therefore, a heterogeneous Fenton reaction has been developed to function at neutral pH. In the present study, the Bio-Fenton reaction was carried out using magnetite ($Fe(II)Fe(III)_2O_4$) and H_2O_2 generated by a newly isolated H_2O_2-producing bacterium, *Desemzia* sp. strain C1 at pH 6.8 to degrade chloroacetanilide herbicides. The optimal conditions for an efficient Bio-Fenton reaction were 10 mM of lactate, 0.5% (w/v) of magnetite, and resting-cells ($O.D._{600} = 1$) of strain C1. During the Bio-Fenton reaction, 1.8–2.0 mM of H_2O_2 was generated by strain C1 and promptly consumed by the Fenton reaction with magnetite, maintaining stable pH conditions. Approximately, 40–50% of the herbicides underwent oxidation through non-specific reactions of •OH, leading to dealkylation, dechlorination, and hydroxylation via hydrogen atom abstraction. These findings will contribute to

* Corresponding author.
** Corresponding author.
E-mail addresses: hghur@gist.ac.kr (H.-G. Hur), youriyang25@kangwon.ac.kr (Y. Yang).

https://doi.org/10.1016/j.chemosphere.2024.141912
Received 22 February 2024; Received in revised form 3 April 2024; Accepted 4 April 2024
Available online 4 April 2024

advancing the Bio-Fenton system for non-specific oxidative degradation of diverse organic pollutants under *in-situ* environmental conditions with bacteria producing high amount of H_2O_2 and magnetite under a neutral pH condition.

1. Introduction

The conventional Fenton/Fenton-like reaction has been extensively employed for the elimination of environmental pollutants, owing to its simplicity that involves readily available reactants such as hydrogen peroxide (H_2O_2) and Fe(II or III) sources. Notably, this method eliminates the necessity for special equipment such as UV light sources and ozone generators, distinguishing it from other advanced oxidation processes. During the Fenton reaction, three primary reactive oxygen species (ROS) are predominantly generated, including hydroxyl radicals (•OH), hydroperoxyl radicals/superoxide anions (•OOH and $\bullet O_2^-$), and high-valent iron oxo (Fe(IV)═O), which could be from the catalytic decomposition of H_2O_2 (Heet al. 2016). Among these ROS, •OH stands out with the highest redox potential of 2.80 eV, allowing it to react with almost all recalcitrant organic compounds (Qin et al., 2018).

Despite the apparent simplicity of the Fenton reaction, the mechanisms and efficiency of this reaction are rather complicated. Its performance is notably influenced by diverse factors, including the oxidation state of iron, concentrations of reactants, and the properties of ligands and buffers (Chen, 2019). Additionally, the presence of natural radical scavengers in the reaction system may diminish the chances of attacking targeted organic compounds by capturing the radicals. Significantly, the availability of iron in the Fenton reaction might be the most critical determinant, influencing the overall efficiency of the reaction. In other words, the pH of the system plays a critical role, as it is closely linked to the solubility of iron.

The Fenton reaction can be described as equations (1)–(4) (Korpe et al., 2022) in which oxidation reactions, neutralization, coagulation for precipitation and pH should be considered to proceed the forward reactions. Specifically, the reaction between Fe(II) and H_2O_2 favors an acidic pH < 3, thereby promoting rapid •OH generation. The pollutants (R) would be degraded by •OH with the formation of Fe(III) sludge. The limitations of lowering pH in the conventional Fenton/Fenton-like systems make their *in-situ* application for degrading pollutants impractical. Consequently, alternative approaches have been explored to enhance iron solubility and prevent precipitation at circumneutral pH.

$$H_2O_2 + Fe(II) \rightarrow Fe(III) + OH^- + \bullet OH \quad (1)$$

$$RH + \bullet OH \rightarrow \bullet R + H_2O \quad (2)$$

$$\bullet R + Fe(III) \rightarrow R^+ + Fe(II) \quad (3)$$

$$Fe(II) + \bullet OH \rightarrow Fe(III) + OH^- \quad (4)$$

In the environment, iron can exist in two oxidation states: ferrous (Fe (II)) or ferric (Fe(III)), which is highly related to the surrounding pH and E_h conditions. The majority of iron tends to exist in solid mineral forms rather than in a dissolved state due to natural hydrolysis and oxidation. This is because the pH in the natural environment is typically not low enough to prevent the formation of hydroxides under oxidizing conditions (Hem and Cropper, 1962). Consequently, in circumneutral environments, the predominant form of iron is usually deposited as poorly crystalline Fe(III) minerals, such as hydrated iron (III) oxides, $Fe(OH)_3$ and ferrihydrites. This process often results in the formation of various iron mineral phases, predominantly hematite ($Fe(III)_2O_3$) and magnetite ($Fe(II)Fe(III)_2O_4$) in these environments, based on redox and geochemical conditions (Schwertmann and Cornell, 2000; Kappler and Straub, 2005; Park et al., 2018). Particularly at redox interfaces, such as in subsurface sediments, even microbial processes of Fe(II) oxidation or Fe (III) reduction can contribute to the formation of magnetite, a representative mixed-valence iron oxide mineral (Kappler and Newman, 2004; Lee et al., 2008; Piepenbrock et al., 2011).

Recently, heterogeneous Fenton reactions have been investigated by using these iron oxides as catalysts for more practical and efficient applications. These approaches are particularly intriguing as they can be executed at circumneutral pH and, more importantly, the iron catalysts such as hematite ($Fe(III)_2O_3$), goethite (Fe(III)O(OH)), and magnetite ($Fe(II)Fe(III)_2O_4$) could be repetitively reused during the reactions (He et al., 2016; Li et al., 2015; Panda et al., 2011; Xu and Wang, 2012). Notably, magnetite emerges as a highly efficient catalyst due to its outstanding properties. Magnetite is a mixed-valence iron oxide with a formula of $Fe(III)_{tet}Fe(II/III)_{oct}O_4^{2-}$ at room temperature. Ideally, magnetite has tetrahedral and octahedral sites in its inverted cubic spinel structure that are occupied by Fe(III) cation and equal numbers of Fe(II) and Fe(III) in the tetrahedral sites and the octahedral sites, respectively (Doriguetto et al., 2003; He et al., 2016). The presence of Fe (II) and Fe(III) in the octahedral sites plays a role similar to peroxidase, accelerating the Fe(II)/Fe(III) cycle and enhancing •OH generation following equation (1) (Chen et al., 2020; He et al., 2016; Larkin et al., 2007). In addition, magnetite exhibits low iron leachate and high stability under neutral conditions (He et al., 2016). Furthermore, the magnetic property of magnetite would facilitate simple and rapid recollection after the reaction, enabling its reuse for subsequent reactions (Munoz et al., 2015).

In our previous studies, the Bio-Fenton reaction using H_2O_2 generated from glucose oxidase (GOx) of *Aspergillus niger* was carried out to degrade environmental pollutants including sulfonated polyethylene, herbicides, and bisphenol A in the presence of Fe(III)-citrate at pH 5.5 (An et al., 2023; Ghatge et al., 2022; Yang et al., 2022). The Bio-Fenton reaction demonstrated significant potential for *in-situ* applications, eliminating the necessity to transport wastes to removal sites and thereby making the remediation process easier and more time-efficient. While this departure from the traditional Fenton process provided a better understanding of the Fenton system, the challenges associated with pH and iron precipitation remained unresolved.

Alachlor, a prominent member of chloroacetanilide herbicides, has been extensively used in the U.S. from its registration in 1969 until the mid-1990s, with an annual usage of 55–60 million pounds (EPA, 1998). However, the use of alachlor has been restricted in the U.S. due to its acute toxicity, carcinogenicity, and reproductive toxicity to animals (Lerro et al., 2018). Following the limitations on alachlor, other chloroacetanilide herbicides like acetochlor and metolachlor were developed and widely adopted in agriculture. In detail, acetochlor and metolachlor have consistently ranked up top 3rd-7th in the active ingredients in the most commonly used conventional pesticides in the U.S. agricultural market sector over the last two decades (Atwood and Paisley-Jones, 2017). However, the extensive use of these herbicides has led to contamination in soil and water. In particular, alachlor exhibits high water solubility (0.24 g/L at 25 °C) due to the polarity of carbonyl and ether groups in chemical structure, and low persistence in aerobic soil, with a moderate degradation rate and a half-life of 2–3 weeks (EPA, 1998). Consequently, its high mobility and low adsorption on organic matter raises concerns about leaching to groundwater and potential hazards to humans and animals. Taken together, it should be considered that the *in-situ* degradation of residual chloroacetanilide herbicides to prevent further contamination into environments.

In the present study, the Bio-Fenton system has been improved by applying H_2O_2-producing bacterium and magnetite ($Fe(II)Fe(III)_2O_4$) as Fenton reactants at pH of 6.8. During the reaction, three chloroacetanilides herbicides, acetochlor, alachlor, and metolachlor, were employed as representative organic compounds. Throughout the

reaction, the amount of H_2O_2, residual compounds, and •OH was measured to examine the efficiency of the Bio-Fenton degradation. Additionally, a possible degradation pathway was proposed by the identification of products resulting from the non-specific Bio-Fenton degradation reactions. This innovative strategy suggested in the present study could shed light on the application potential of the biological system at practical environmental conditions for *in-situ* contamination removal.

2. Materials and methods

2.1. Chemicals and media

Acetochlor (ACC, 2-chloro-*N*-(ethoxymethyl)-*N*-(2-ethyl-6-methylphenyl)acetamide, 96%), alachlor (ALC, 2-chloro-*N*-(2,6-diethylphenyl)-*N*-(methoxymethyl)acetamide, 99%), and metolachlor (MTC, 2-chloro-*N*-(2-ethyl-6-methylphenyl)-*N*-(2-methoxy-1-methylethyl) acetamide, 97%), hematite ($Fe(III)_2O_3$, <5 μm, 96%), goethite (Fe(III)O(OH), 30–63% Fe), and magnetite ($Fe(II)Fe(III)_2O_4$, <5 μm, 95%), ferric chloride hexahydrate ($FeCl_3{\cdot}6H_2O$), and potassium hexacyanoferrate ($K_3Fe(CN)_6$), sodium sulfate (Na_2SO_4), 2-deoxyribose, trichloroacetic acid, and 2-thiobarbituric acid were purchased from Sigma-Aldrich (St. Louis, MO). H_2O_2 (30%, w/v) was purchased from Daejung Chemicals & Metals (Siheung, Republic of Korea). Brain Heart Infusion (BHI) medium was purchased from Difco. (Detroit, MI).

High-purity grade dichloromethane, ethyl acetate, and methanol were purchased from Thermo Fisher Scientific (Waltham, MA). Amplex® Red Hydrogen Peroxide/Peroxidase Assay Kit was purchased from Invitrogen (Carlsbad, CA). Each chloroacetanilide herbicide was freshly prepared in methanol prior to the experiments. Mineral salts medium (MSM) was composed $Na_2HPO_4{\cdot}7H_2O$ (5.2 g/L), KH_2PO_4 (2.7 g/L), KOH (0.14 g/L), nitrilotriacetic acid (0.2 g/L), $MgSO_4{\cdot}7H_2O$ (0.5 g/L), $CaCl_2{\cdot}2H_2O$ (0.06 g/L), $(NH_4)_6Mo_7O_{24}{\cdot}4H_2O$ (0.18 mg/L), $(NH_4)_2SO_4$ (0.1 g/L), and trace metals (Stanier et al., 1966). Prussian blue (PB) agar plate was prepared as previously described by Saito et al. (2007).

2.2. Isolation and identification of H_2O_2-producing bacterium

An oil-contaminated soil sample was collected from auto repair shops in Gwangju, South Korea, where the soil had been consistently exposed to waste oil debris from the car fixation process. One percent of soil (w/v) was added into 25 mL MSM, and suspended at 30 °C and 150 rpm for 1 h. Subsequently, the liquid phase was serially diluted, and 0.1 mL of each dilution was spread on PB agar plates to screen H_2O_2-producing bacteria by observing the development of blue precipitates. Pure bacterial isolates were obtained through sequential streaking on PB agar plates, and their H_2O_2 production capabilities were assessed by quantifying H_2O_2 during bacterial growth in BHI liquid medium. The strain exhibiting the highest H_2O_2 production was finally selected for further experiments, which was named as strain C1. Strain C1 was deposited to Korean Collection for Type Cultures (KCTC) as the deposit number of KCTC 18996BP. To compare cell growth and H_2O_2 production, representative H_2O_2-producing bacteria such as *Desezma incerta* KCTC 3258^T, *Streptococcus oralis* subsp. *oralis* KCTC 13048^T, and *Aerococcus viridans* KCTC 3485^T were purchased from KCTC.

The 16S rRNA genes of strain C1 were amplified by polymerase chain reaction (PCR), using universal primers, 27F 5′-AGAGTTTGATCCTGGCTCAG-3′ and 1492R 5-GGTTACCTTGTTACGACTT-3′, and sequenced in Macrogen (Daejeon, Republic of Korea). The 16S rRNA gene sequence was compared with the sequences of type strain using NCBI-BLAST (https://blast.ncbi.nlm.nih.gov/Blast.cgi.) (Johnson et al., 2008). Phylogenetic tree was reconstructed using MEGA software version 7.0 after multiple alignment by Clustal W (Larkin et al., 2007). Neighbor-joining algorithm was used to determine the phylogeny of strain C1 with the Kimura-2 parameter model and 1000 iterations of bootstrap sampling (Kimura, 1980; Saitou and Nei, 1987). Additionally, the draft genome sequence of strain C1 was constructed based on the PacBio sequencing data and deposited in GenBank under the BioProject accession number PRJNA777376 (Ko et al., 2022).

2.3. Optimization conditions for efficient Bio-Fenton degradation of chloroacetanilide herbicides using Desemzia sp. strain C1

Prior to biological experiments using strain C1, abiotic Fenton reaction was conducted using externally supplied H_2O_2 and three different types of iron oxide minerals such as hematite ($Fe(III)_2O_3$), goethite (Fe(III)O(OH)), and magnetite ($Fe(II)Fe(III)_2O_4$) to select the most favorable iron source for the efficient Bio-Fenton reaction. The Fenton reaction was carried out in 150 mL serum bottles sealed with Teflon-lined rubber septa and aluminum caps, containing 30 mL of MSM adjusted to pH 6.8, 1.5 mM of H_2O_2, 0.5% (w/v) of each iron source, and 0.1 mM ALC as a representative chloroacetanilide herbicide. The reaction proceeded at 30 °C and 120 rpm until H_2O_2 completely disappeared. The effect of each iron source on the Fenton reaction was evaluated by measuring the residual H_2O_2 and ALC concentration throughout the reaction. Magnetite showed the fastest consumption of H_2O_2 during the Fenton reaction; consequently, it was selected as the preferred iron source for further experiments.

The optimal substrate for the maximum H_2O_2 production by the resting-cells ($O.D._{600} = 1$) of strain C1 was examined by using 10 mM of different substrates such as glucose, pyruvate, lactate, and oxalate, which are well-known substrates for H_2O_2-producing enzymes in bacterial metabolism (Burrell et al., 2007; Kleppe, 1966; Taniai et al., 2008). Among these, lactate exhibited the highest level of H_2O_2 production by strain C1, thus it was selected as the final substrate for further experiments.

The Bio-Fenton reaction was performed under the same conditions to the abiotic Fenton reaction except H_2O_2 was internally provided by the resting-cells ($O.D._{600} = 1$) of strain C1 using lactate. A single colony of strain C1 was initially inoculated into BHI liquid medium and incubated at 30 °C without agitation for 24 h. Subsequently, 1% (v/v) of the culture was transferred to a fresh BHI medium and incubated for 48 h under the same conditions. Cells were harvested at the mid-exponential phase through centrifugation at 9,000×*g* at 4 °C for 10 min. Then, the cells were washed twice with MSM and resuspended with fresh medium for the resting-cell experiments.

The optimal concentration of magnetite for the Bio-Fenton degradation was investigated using various concentrations at 0.1%, 0.5%, and 1.0% (w/v). In addition, ALC as a representative chloroacetanilide herbicide was added to the reaction at 0.1 mM as the final concentration. Simultaneously, the control samples were prepared as follows: (1) ALC, (2) strain C1 and ALC, (3) heat-killed strain C1 and ALC, (4) magnetite and ALC, (5) strain C1 and magnetite. All control samples contained 10 mM of lactate as a substrate. The reaction was performed at 30 °C and 120 rpm until H_2O_2 in the Bio-Fenton reaction samples completely disappeared. During the reaction, 0.6 mL of the reaction mixture was periodically sampled to measure pH, residue of H_2O_2 and ALC, amount of •OH, and chloride ion (Cl^-) possibly released from ALC. After every sampling, the measurements of pH and •OH were immediately carried out. The samples were ten-fold diluted with sterile deionized water and used for measuring pH using pH meter (Orion Star™ A211, Thermo Fisher Scientific). Meanwhile, the residual H_2O_2 was qualitatively checked by dropping a small amount of the sample on PB agar plates until H_2O_2 disappeared as an indicator of the Fenton reaction with magnetite. A 0.1 mL of aliquot was kept separately at −20 °C for H_2O_2 quantification. The rest of reaction sample was heated at 65 °C for 15 min to inactivate the bacterial activity and then stored at 4 °C for the analysis of residual ALC and its degradation products. All experiments were carried out in triplicate.

The similar biodegradation tests to other chloroacetanilide herbicides, ACC and MTC, were investigated at 0.1 mM of the final

concentration according to the same procedure used in the Bio-Fenton degradation for ALC. All experiments were carried out in triplicate.

2.4. Quantification of residue of H_2O_2 and herbicides, amount of •OH, and Cl^- ion during Bio-Fenton degradation

The residual H_2O_2 during the Bio-Fenton reaction was quantified using an Amplex® red hydrogen peroxide/peroxidase assay kit of Invitrogen (Carlsbad, CA) according to the manufacturer's instructions. The amount of H_2O_2 was calculated based on a standard curve of H_2O_2 ranging from 1 to 5 μM ($R^2 = 0.99$).

To quantify the residual herbicides during the Bio-Fenton reaction, 0.4 mL of the samples was extracted twice with a ten-fold volume of dichloromethane. The organic phase was passed through an anhydrous Na_2SO_4 to remove the aqueous phase, followed by evaporation using a speedvac vacuum concentrator (Thermo Fisher Scientific). The extract was dissolved in 0.4 mL of methanol and followed by filtering with polyvinylidene fluoride (PVDF) syringe filter (Whatman-GE Healthcares, Pittsburgh, PA) before high-performance liquid chromatography (HPLC) analysis. HPLC was equipped with a photodiode array detector (PDA) (Agilent, Santa Clara, CA) and a reverse-phase ODS-2 column (Inertsil™, 4.6 × 250 mm, 5 μm in particle size) (GL Sciences, Tokyo, Japan) which was kept at 40 °C during the operation. The isocratic elution was operated at the ratio of 50%:50% of solvent A (deionized water containing 0.1% formic acid) and solvent B (acetonitrile) at the flow rate of 1 mL/min. The three chloroacetanilide herbicides, ACC, ALC, and MTC, were separately monitored at 205 nm and quantified based on a standard curve drawn using different concentrations of each herbicide ranging from 0.05 to 0.2 mM ($R^2 > 0.99$).

The amount of •OH during the Bio-Fenton reaction was estimated by measuring thiobarbituric acid reactive substance (TBARS) generated from 2-deoxyribose in the presence of •OH (Halliwell and Gutteridge, 1981; Krueger et al., 2015). Shortly, 2-deoxyribose was added to 0.5 mL of the reaction mixture at a concentration of 2.8 mM, followed by reaction at 30 °C and 120 rpm for 2 h. Afterward, 0.25 mL of trichloroacetic acid (2.8%, w/v) and 0.25 mL of 2-thiobarbituric acid (1%, w/v) in 50 mM NaOH were added to the mixture and reacted at 95 °C for 15 min. After cooling, the absorbance of TBARS was measured at 530 nm using UV–Vis spectrophotometer (Optizen™ POP, Daejeon, Republic of Korea). Blank sample, which contained sterile deionized water instead of 2-deoxyribose, was subtracted for more precise calculation of the final absorption values.

The amount of Cl^- ions during the Bio-Fenton reaction was determined using ion chromatography (IC) system equipped with a conductivity detector (ICS-5000+, Thermo Dionex). To separate anions in the samples, an AS19 column (4 × 250 mm, Thermo Dionex) maintained at 45 °C was used with a Thermo Dionex ADRS 600 dynamically regenerated suppressor (4 mm). The mobile phase was Eluent Generator Cartridge KOH solution (Thermo Fisher Scientific), and the flow rate was 1.0 mL/min. Data analysis was performed using the Chromeleon 7.0. For the quantification of Cl^- ion in the samples, standard Cl^- ion solution ranging from 1 to 100 μM was prepared in MSM ($R^2 > 99.9$).

2.5. Identification of products from Bio-Fenton degradation of chloroacetanilide herbicides using GC/MS analysis

The products from the Bio-Fenton degradation of three chloroacetanilide herbicides (ACC, ALC, MTC) were identified using gas chromatography-mass spectrometry (GC-MS). Bio-Fenton reaction samples (15 mL) after 5 d of reaction was vigorously extracted with ten-fold volumes of dichloromethane. The organic phase was collected after passing through an anhydrous Na_2SO_4 to remove the aqueous phase, and evaporated using a rotary evaporator (EYELA, NY). The extract was dissolved in 1 mL of dichloromethane and filtered using a PVDF syringe filter, and immediately analyzed using GC-MS.

GC-MS analysis was performed using 7890A Gas Chromatography coupled with a 5975C mass selective detector and a HP 7693A injector (Agilent). The analysis conditions were as follows: DB-5MS Ultra Inert fused silica capillary column (30 m × 0.25 mm (i.d.), 0.25 μm film thickness, Agilent); helium as carrier gas with the flow rate of 1.0 mL/min; oven temperature, 50 °C for 1 min, then elevated to 180 °C with a rate of 30 °C/min and held for 10 min, and elevated to 280 °C with a rate of 10 °C/min, and finally held at 280 °C for 10 min; temperature of the injector and transfer line, 280 °C; split the injection mode with a split ratio of 2:1; solvent delay at 2.5 min; mass scan range from *m/z* 50 to 350; ionization voltage, 70 eV; source temperature, 230 °C; MS quadrupole temperature, 150 °C. Possible structures of the products were predicted via the overall consideration of the following information: (I) *m/z* values, (II) chlorine atom isotope patterns, (III) NIST spectra library, and (IV) mass spectra interpretation.

3. Results and discussion

3.1. Isolation and identification of H_2O_2-producing bacterium from oil-contaminated soil

H_2O_2-producing bacteria were screened from the oil-contaminated soil by observing blue-color precipitates around colonies on PB agar plates, which indicated the presence of H_2O_2 produced from bacteria (Saito et al., 2007). After 2 d of incubation, a colony exhibiting a strong blue-color was selected and named as strain C1 (Fig. 1A). The 16S rRNA gene sequence of strain C1 showed the highest similarity with *Desemzia incerta* DSM 20581^T (99.29%), followed by *Pisciglobus halotolerans* C01^T (96.47%) and *Carnobacterium inhibens* subsp. *gilichinskyi* WN1359^T (95.33%). The phylogenetic tree built based on the 16S rRNA sequences revealed that strain C1 clustered with the *Desemzia* genera (Fig. 1B). Therefore, strain C1 was identified as *Desemzia* sp. strain C1.

Desemzia genera are characterized in Bergey's Manual as gram-positive, non-spore forming, microaerophilic, and catalase negative bacteria (Stackebrandt, 2015). Although strain C1 exhibited physiological and cultural characteristics resembling well-known H_2O_2-producing bacteria such as *Streptococcus*, *Lactobacillus*, *Bifidobacterium*, and *Pediococcus*, it was not clustered with these genera (Barnard and Stinson, 1999; Hertzberger et al., 2014). Furthermore, there have been no reports on the pathogenicity of *Desemzia* genera since the first report on the *Desemzia incerta* by Steinhaus in 1941 (Steinhaus, 1941). A comparative analysis of growth and H_2O_2 production of strain C1 was conducted with other representative H_2O_2-producing bacteria, including *Desemzia incerta*, *Streptococcus oralis*, and *Aerococcus viridans*. It found that strain C1 showed better growth and H_2O_2 production capability than others in BHI medium (Fig. S1). Strain C1 exhibited optimal growth at 30 °C under static conditions, and reached its highest value of 0.8 at 40 h (Fig. S1A). H_2O_2 concentration produced by strain C1 gradually increased to 0.45 mM until 120h of incubation. Subsequently, it rapidly rose by approximately 0.2 mM at 160 h of incubation (Fig. S1B). Consequently, strain C1 could be considered a novel and promising H_2O_2 supplier for the Bio-Fenton reaction.

3.2. Optimization of abiotic Fenton reaction for Bio-Fenton reaction

Prior to the Bio-Fenton degradation experiments using *in-situ* generated H_2O_2 by strain C1, the effect of different iron oxides on the abiotic Fenton reaction at pH 6.8 was investigated with externally supplied H_2O_2. The efficiency in the presence of different iron oxides was assessed by determining degradation of ALC as a representative herbicide among chloroacetanilide herbicides. The better Fenton degradation efficiency toward ALC was found with iron oxides in the order of magnetite > goethite > hematite (Fig. 2). Most of the supplied H_2O_2 was consumed within 1 d by the Fenton reaction with magnetite. Meanwhile, H_2O_2 was gradually consumed and completely disappeared at 5 d in the presence of goethite. Notably, the H_2O_2 consumption rate was the slowest in the presence of hematite with about 50% remained

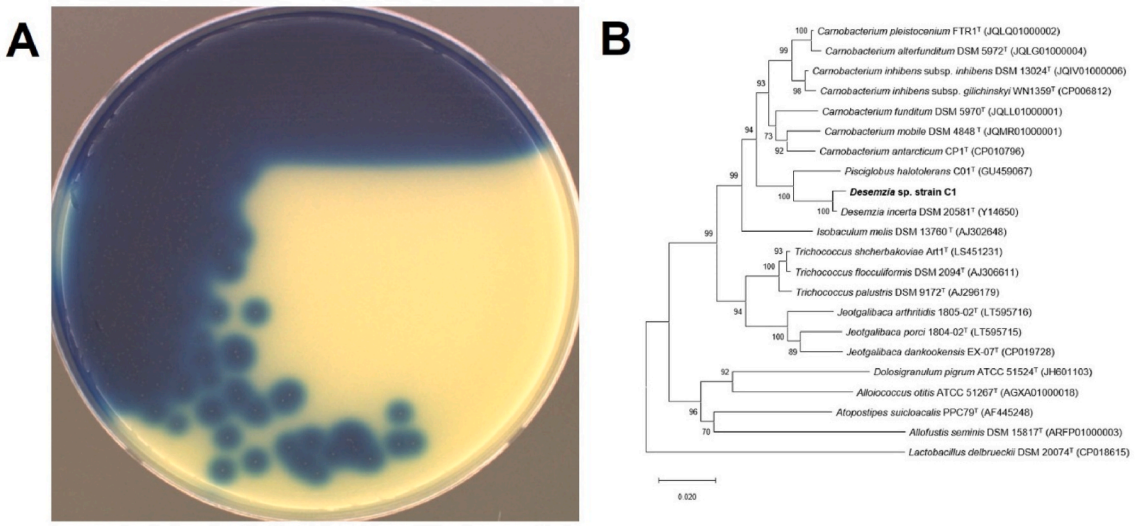

Fig. 1. Isolation of hydrogen peroxide (H_2O_2)-producing bacterium, *Desemzia* sp. strain C1, on Prussian blue (PB) agar plate (A) and the phylogenetic tree of strain C1 (B). Blue precipitates on the PB agar plate indicate the presence of H_2O_2. (For interpretation of the references to color in this figure legend, the reader is referred to the Web version of this article.)

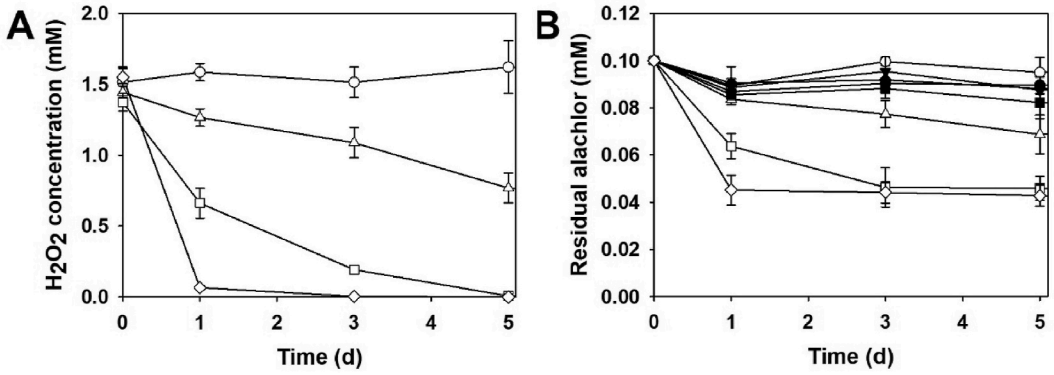

Fig. 2. Effect of different iron oxides (hematite, goethite, and magnetite) on the abiotic Fenton degradation of alachlor (ALC). The reaction mixture was composed of 1.5 mM hydrogen peroxide (H_2O_2), 0.5% (weight/volume) of each iron oxide, and 0.1 mM ALC. ALC (-●-), H_2O_2+ ALC (-○-), hematite + ALC (-▼-), hematite + H_2O_2+ ALC (-△-), goethite + ALC (-■-), goethite + H_2O_2+ ALC (-□-), magnetite + ALC (-◆-), magnetite + H_2O_2+ ALC (-◇-). Values represent the mean of triplicate determinations ± standard deviation.

unconsumed at 7 d of reaction. The order of ALC degradation in the presence of different iron oxides coincided with the H_2O_2 consumption rate. Approximately 60% of ALC was degraded within 1 d of reaction in the presence of magnetite, followed by remaining the rest of it by the end of reaction. Meanwhile, ALC degradation reached 40% and 20% within 1 d in the presence of goethite and hematite, respectively. Further incubation in the presence of goethite and hematite showed degradation of ALC up to 60% and 30%, respectively.

The efficiency of the Fenton reaction can be influenced by various factors related to the types of heterogeneous iron oxides, such as their density, porosity, pore size and distribution, volume, and surface area (Solís-López et al., 2014). Primarily, the structural differences among iron oxides could play a significant role. Magnetite, for instance, has tetrahedral and octahedral sites occupied by Fe(III) cation and mixture of Fe(II)/Fe(III), respectively (Doriguetto et al., 2003; He et al., 2016). In other words, the octahedral site of magnetite would be a very versatile redox site capable of accommodating both Fe(II) and Fe(III), allowing for easy reduction of Fe(III) to Fe(II) without structural constraints. Therefore, this unique structure may render magnetite a more efficient catalyst for the Fenton reaction with H_2O_2, contributing to a higher degradation of ALC compared to other iron oxides under the same conditions. In accordance with these results, it has been reported that magnetite-catalyzed Fenton reactions exhibit higher •OH production due to a faster reaction rate between H_2O_2 and Fe(II) sites compared to goethite and hematite (Solís-López et al., 2014; Zhao et al., 2018). Consequently, magnetite was selected as the better iron source for further Bio-Fenton reactions than hematite and goethite.

3.3. Optimal conditions for Bio-Fenton reaction using the resting-cells of *Desemzia* sp. strain C1

The effect of different substrates on H_2O_2 production from the resting-cells of strain C1 was investigated for the further Bio-Fenton degradation experiments. H_2O_2 concentration produced from the resting-cells of strain C1 was approximately 0.8 mM and 1.8 mM in the presence of glucose and lactate, respectively (Fig. 3). This suggests that lactate is likely to produce H_2O_2 than glucose in strain C1. In bacterial metabolism, H_2O_2 is primarily generated in central and energy metabolism by various oxidases, such as pyruvate oxidase (POx), lactate oxidase (LOx), glucose oxidase (GOx), NADH oxidase (NOx), etc (Condon, 1987). Therefore, it can be inferred that the main enzymatic reactions for H_2O_2 production in strain C1 are likely mediated by LOx. Consequently, lactate was selected as the substrate for inducing H_2O_2-producing enzymes in strain C1. Additionally, the amount of H_2O_2

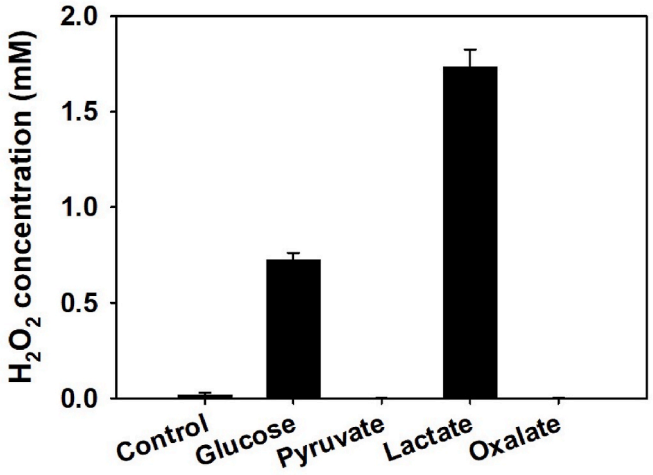

Fig. 3. Hydrogen peroxide (H_2O_2) production by *Desemzia* sp. strain C1 in the presence of each 10 mM substrates (glucose, pyruvate, lactate, and oxalate) under the resting-cell condition ($O.D._{600}$ = 1) at 24 h incubation. Values represent the mean of triplicate determinations ± standard deviation.

produced by strain C1 was compared to other representative H_2O_2-producing bacteria mediated by LOx such as *Desemzia incerta*, *Streptococcus oralis*, and *Aerococcus viridans* under the resting-cell experiments ($O.D._{600}$ = 1) in the presence of lactate. Strain C1 exhibited the highest H_2O_2 production among them (Fig. S2).

The Bio-Fenton degradation of ALC was investigated with different concentrations of magnetite ranging from 0.1% to 1.0%. The reaction efficiency was assessed by measuring pH, H_2O_2 consumption rate, and ALC degradation (Fig. 4). Termination of the Bio-Fenton reaction was determined when the residual H_2O_2 was no longer detected on the PB agar plate (Fig. S3). The initial pH in the reaction mixture was 6.8, at which strain C1 grows well. Fig. 4A shows that pH in the reaction mixture was sustained by the end of incubation regardless of the concentrations of magnetite. It should be noted that the current Bio-Fenton system working at the neutral pH conditions take advantages of diminishing the issues of iron insolubility and H_2O_2 instability at high pH, which lead to iron precipitation, sludge disposal, and inefficient Fenton reactions.

Strain C1 produced 1.8–2.0 mM of H_2O_2 in the presence of 10 mM lactate within 2 d, which remained constant for 5 d of incubation in the absence of magnetite (Fig. 4B). However, as compared to the control culture medium, the Bio-Fenton culture medium with strain C1 in the presence of magnetite only contained 25–50% H_2O_2 of the control at 1 d, followed by steady decrease by 5 d of incubation. This phenomenon may

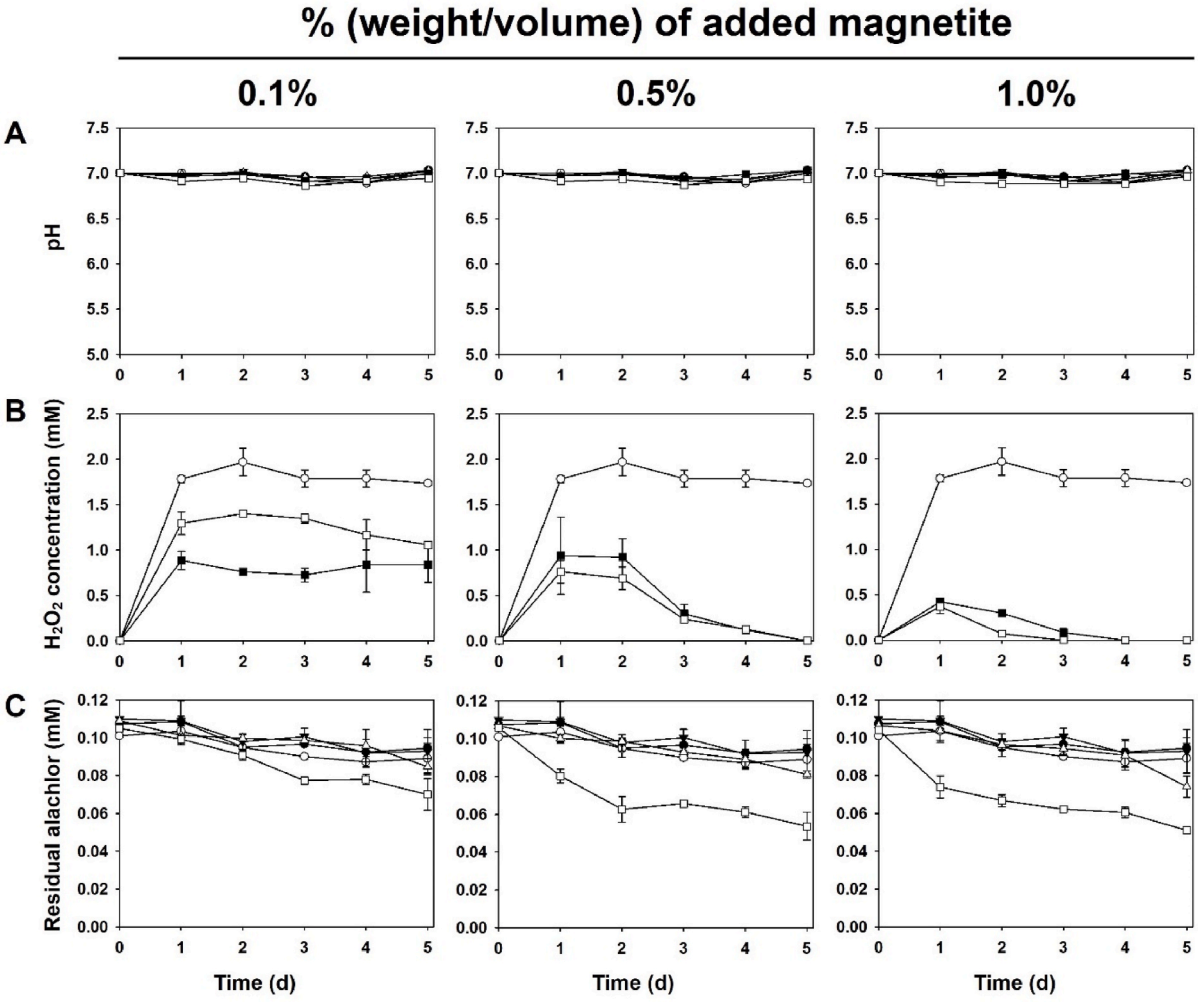

Fig. 4. Measurement of pH (A), hydrogen peroxide (H_2O_2) concentration (B), and residual alachlor (ALC) (C) during Bio-Fenton degradation by the resting-cells of strain C1 in the presence of different amounts of magnetite ($Fe(II)Fe(III)_2O_4$) at 0.1%, 0.5%, and 1.0% (weight/volume) for 5 d of incubation. ALC (-●-), C1 + ALC (-○-), heat-killed C1 + ALC (-▼-), magnetite + ALC (-△-), C1 + magnetite (-■-), C1 + magnetite + ALC (-□-). Values represent the mean of triplicate determinations ± standard deviation.

result from the immediate consumption of H_2O_2 by Bio-Fenton reaction between *in-situ* generated H_2O_2 from strain C1 and magnetite. In particular, the H_2O_2 consumption rate was likely to be dependent on the concentrations of magnetite. The complete H_2O_2 consumption in the Bio-Fenton reaction with 0.1%, and 0.5% and 1.0% magnetite took 10 d, and 4–5 d, respectively (Fig. S4). In addition, the effect of substrate ALC on the time to reach the complete H_2O_2 consumption was shown to delay the consumption rate.

The Bio-Fenton degradation rate of ALC increased as the concentrations of magnetite increased from 0.1% to 1.0% (Fig. 4C). In detail, 1 d of incubation for the Bio-Fenton reaction degraded up to 5–30%, followed by gradual decline by the end of incubation regardless of magnetite concentrations. Taken together, 1.0% of magnetite seemed to be the most efficient concentration for the reaction, considering pH, H_2O_2 consumption, and the residual amount of ALC during the Bio-Fenton degradation using strain C1. However, 0.5% of magnetite was selected as the optimal iron concentration for further Bio-Fenton reaction, taking into the similar degradation efficiency between 0.5% and 1.0% of magnetite. Thus, the optimal conditions for the Bio-Fenton degradation of chloroacetanilide herbicides were determined as 10 mM of lactate and 0.5% (w/v) of magnetite, and pH 6.8 using the resting-cells (O.D.$_{600}$ = 1) of *Desemzia* sp. strain C1.

3.4. Bio-Fenton degradation of chloroacetanilide herbicides using the resting-cells of Desemzia sp. strain C1

The Bio-degradation experiments of ACC and MTC was performed, according to the same methods applied in the Bio-Fenton degradation for ALC. Similarly, the culture of strain C1 in the presence of magnetite and ACC showed about 1.5 mM of H_2O_2 produced in 1 d of incubation, followed by complete consumption in 6 d of incubation (Fig. 5A). ACC in the culture of strain C1 with magnetite was degraded up to 40% in 1 d, followed by no further degradation (Fig. 5B). Meanwhile, the culture of strain C1 in the presence of magnetite and MTC showed about 2.0 mM of H_2O_2 produced, and similar degradation rate of MTC in the end of incubation (Fig. 5C and D).

3.5. Quantification of •OH and Cl^- during the Bio-Fenton degradation of chloroacetanilide herbicides using the resting-cells of Desemzia sp. strain C1

The generation of •OH during the Bio-Fenton reaction of ACC, ALC, and MTC was monitored by measuring the absorbance of orange-colored TBARS at 530 nm. In the Bio-Fenton sample containing strain C1 with lactate and magnetite, there was a steady increase in absorbance at 530 nm by 12 h, followed by a steady decrease by 48 h of incubation (Fig. 6A). The decrease in absorbance at 530 nm could indicate the non-specific reaction of •OH with various compounds present in the reaction mixture, including strain C1 cells. The Bio-Fenton sample with each herbicide also showed a similar increase in absorbance at 530 nm by 12 h. However, absorbance at 530 nm sharply decreased in the further incubation up to 48 h of incubation. This suggested a correlation between •OH production and consumption by attacking herbicide (0.1 mM).

The formation of ROS with a more powerful redox potential is quite of importance in the application of the Fenton system to the non-selective degradation of pollutants. In Fenton reactions, relatively mild acidic pH conditions above pH 3 is favor to form a high-valent iron oxo (Fe(IV)=O) as a major ROS, while stronger pH conditions below pH 3 provide environments to form •OH (Bataineh et al., 2012; Hug and Leupin, 2003). In our experimental conditions even at neutral pH, however, we found that the resulting ROS shifts to •OH. According to the study on density functional theory (DFT), the iron ions are highly coordinated by phosphate ions in phosphate buffer, which leads to

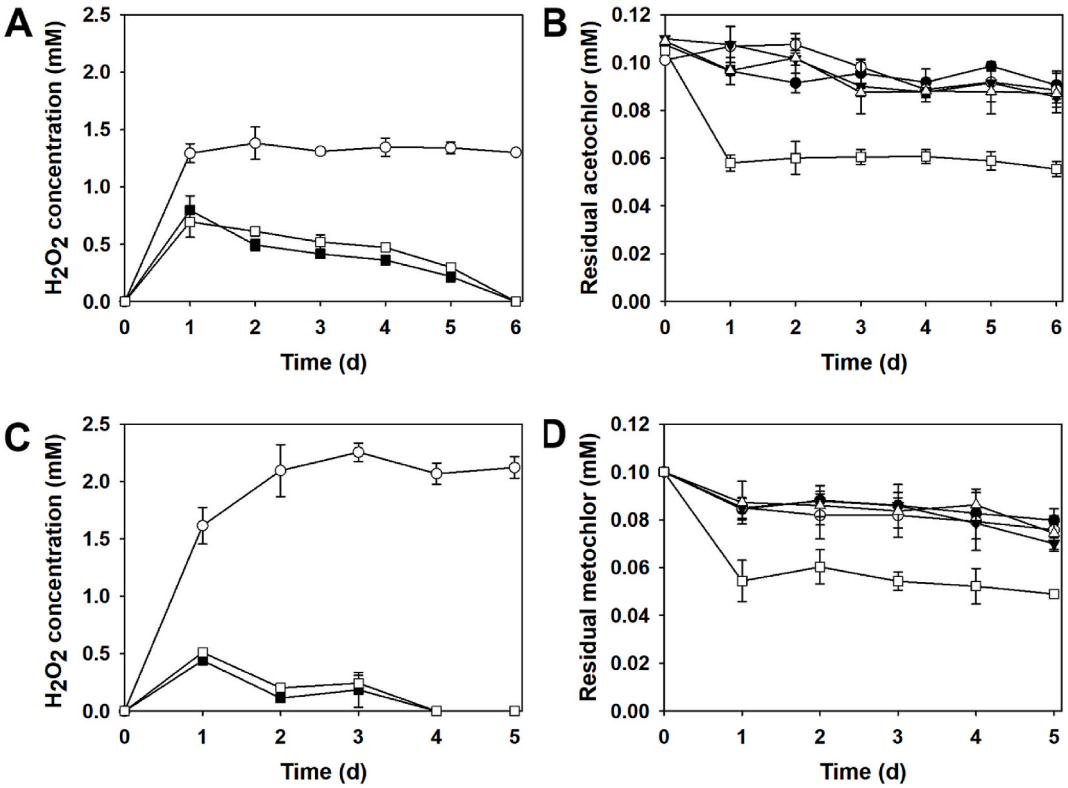

Fig. 5. Production of hydrogen peroxide (H_2O_2) during Bio-Fenton degradation of acetochlor (ACC) (A and B) or metolachlor (MTC) (C and D) by the resting-cells of strain C1 in the presence of 0.5% (weight/volume) magnetite. ACC (-●-), C1 + ACC (-○-), heat-killed C1 + ACC (-▼-), magnetite + ACC (-△-), C1 + magnetite (-■-), C1 + magnetite + ACC (-□-). MTC (-●-), C1 + MTC (-○-), heat-killed C1 + MTC (-▼-), magnetite + MTC (-△-), C1 + magnetite (-■-), C1 + magnetite + MTC (-□-). Values represent the mean of triplicate determinations ± standard deviation.

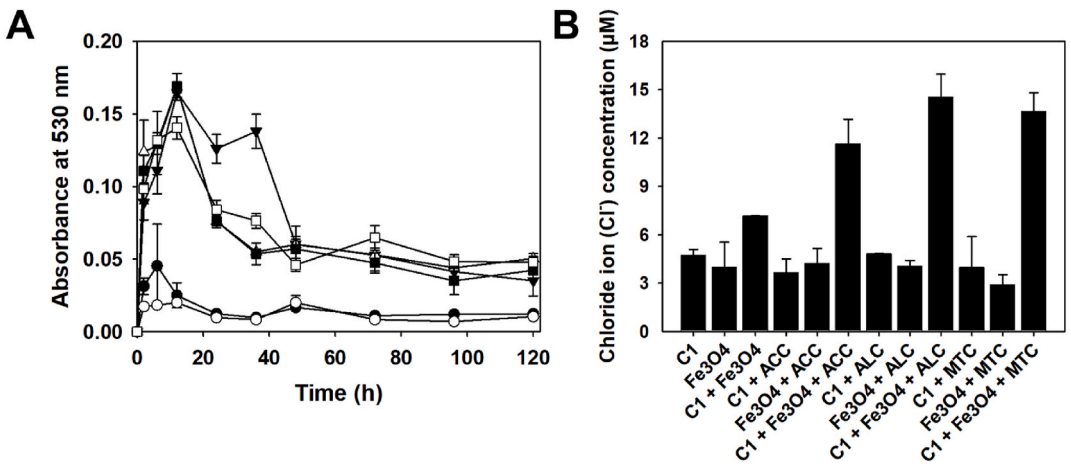

Fig. 6. Measurement of hydroxyl radicals during Bio-Fenton degradation of acetochlor (ACC), alachlor (ALC), and metolachlor (MTC) by the resting-cells of strain C1 in the presence of 0.5% (weight/volume) magnetite (A). C1 (-●-), magnetite (-○-), C1 + magnetite (-▼-), C1 + magnetite + ACC (-△-), C1 + magnetite + ALC (-■-), C1 + magnetite + MTC (-□-). Concentration of chloride ions (Cl^-) produced from the Bio-Fenton degradation of acetochlor (ACC), alachlor (ALC), and metolachlor (MTC) after 5 d of reaction (B). Cl^- was quantified based on the standard curve of Cl^- prepared in mineral salt medium ($R^2 > 99.9$). Values represent the mean of triplicate determinations ± standard deviation.

preventing Fe(III) from coordinating with water molecules and increase of pK_a (Chen, 2019). Thus, the formation of Fe(III)–OH from the reductive decomposition of H_2O_2 by Fe(II) will be inhibited in the phosphate buffer solution. Consequently, the high-valent iron oxo (Fe(IV)═O) species from Fe(III)–OH by hydrogen abstraction reaction with •OH is not likely formed in the phosphate buffer. Therefore, it can be concluded that the major oxidant in the current Bio-Fenton reaction is •OH, which participates in the non-specific hydrogen abstraction reaction to the herbicides.

IC analyses showed that Bio-Fenton degradation of each herbicide produced Cl^- in the range of 12–15 μM, which was 3–4 times higher amounts compared to the control experiments in the range of 3–7 μM of Cl^- production (Fig. 6B). Considerably increased amounts of Cl^- ions compared to the control experiments suggested the occurrence of dechlorination on the chloroacetanilide herbicides by the Bio-Fenton reactions at the neutral pH condition. It should be noted that dechlorination of the chloroacetanilide herbicide reduces biological toxicity of the compounds (Henschler, 1994; Tsyganok and Otsuka, 1999).

3.6. Identification of products from the Bio-Fenton degradation of chloroacetanilide herbicides using the resting-cells of Desemzia sp. strain C1

The products resulting from the Bio-Fenton degradation of the chloroacetanilide herbicides were identified through GC-MS analyses, comparing them with the control samples. The peaks detected only in the Bio-Fenton reaction samples were considered for further identification through the comprehensive consideration of (I) *m/z* values, (II) chlorine atom isotope patterns, (III) NIST spectra library, and (IV) mass spectra interpretation.

Four products were identified from the Bio-Fenton degradation of ACC as follows: (A) 2-ethyl-*N*,6-dimethylaniline ([M] at *m/z* 149.1 and the fragment ions of *m/z* 77.1, 106.1, 134.1), (B) 2-chloro-*N*-(2-ethyl-6-methylphenyl)-*N*-methylacetamide ([M] at *m/z* 225.0 and the fragment ions of *m/z* 148.0, 176.0), (C) *N*-(2-ethyl-6-methylphenyl)-*N*-(hydroxymethyl)acetamide ([M] at *m/z* 207.1 and the fragment ions of *m/z* 89.0, 158.1), (D) (*E*)-*N*-(2-ethyl-6-methylphenyl)formimidic acid ([M] at *m/z* 163.1 and the fragment ions of *m/z* 91.1, 120.1, 148.1) (Fig. S5). Four products were identified from the Bio-Fenton degradation of ALC as follows: (A) 2-chloro-*N*-(2,6-diethylphenyl)-*N*-methylacetamide ([M] at *m/z* 239.1 and the fragment ions of *m/z* 148.1, 162.1, 190.1), (B) 1-((2,6-diethylphenyl)(methyl)amino)ethan-1-ol ([M] at *m/z* 207.1 and the fragment ions of *m/z* 148.1, 163.1, 191.1), (C) *N*-(2,6-diethylphenyl)-2-hydroxyacetamide ([M] at *m/z* 207.1 and the fragment ions of *m/z* 89.1, 133.1), (D) (*E*)-*N*-(2,6-diethylphenyl)formimidic acid ([M] at *m/z* 177.1 and the fragment ions of *m/z* 132.1, 162.1) (Fig. S6). Eight products were identified from the Bio-Fenton degradation of MTC as follows: (A) 2-chloro-*N*-isopropyl-*N*-(o-tolyl)acetamide ([M] at *m/z* 225.1 and the fragment ions of *m/z* 134.1, 176.1, 210.0), (B) 2-ethyl-*N*-(1-methoxypropan-2-yl)-6-methylaniline ([M] at *m/z* 207.1 and the fragment ions of *m/z* 72.1, 120.0), (C) 2-hydroxy-*N*-(2-hydroxy-6-methylphenyl)-*N*-(1-methoxypropan-2-yl)acetamide ([M] at *m/z* 253.1 and the fragment ions of *m/z* 165.1, 197.0), (D) *N*-(1-hydroxypropan-2-yl)-*N*-(o-tolyl)acetamide ([M] at *m/z* 207.1 and the fragment ions of *m/z* 134.1, 148.1), (E) 2-chloro-*N*-(2,6-dihydroxyphenyl)-*N*-(1-methoxypropan-2-yl)acetamide ([M] at *m/z* 273.0 and the fragment ions of *m/z* 152.1, 201.0, 228.4), (F) *N*-(1-methoxypropan-2-yl)-2-methyl-6-vinylaniline ([M] at *m/z* 205.1 and the fragment ions of *m/z* 91.1, 160.1), (G) 2-hydroxy-*N*-(2-hydroxyphenyl)-*N*-(1-methoxypropan-2-yl)acetamide ([M] at *m/z* 239.1 and the fragment ions of *m/z* 165.1, 197.0), (H) 2-hydroxy-*N*-(2-hydroxyphenyl)-*N*-(1-hydroxypropan-2-yl)acetamide ([M] at *m/z* 225.1 and the fragment ions of *m/z* 158.1, 176.1) (Fig. S7). These identifications provided insight into the transformation products generated from the Bio-Fenton degradation of chloroacetanilide herbicides.

3.7. Proposed degradation pathway of chloroacetanilide herbicides by the magnetite-driven Bio-Fenton reaction by Desemzia sp. strain C1

In the Fenton reaction, •OH is considered as the primary oxidant among various ROS due to its excellent redox potential. Indeed, numerous studies have extensively reported the critical role of •OH in the oxidative degradation of diverse pollutants, including agrochemicals, dyes, and pharmaceutical compounds (Friedman et al., 2006; Lian et al., 2017; Patel et al., 2020; Qin et al., 2015). Understanding the degradation mechanism by •OH can be explained mainly through two pathways, where it acts as both an electrophile and a nucleophile. Firstly, •OH is directly introduced to compounds at electron-deficient sites of the compounds, and these hydroxyl compounds are further oxidized. Subsequently, these oxidized compounds transform into quinone groups and ultimately into carboxylic acids. Finally, these carboxylic acids undergo mineralization to CO_2 and H_2O through continuous •OH addition. Secondly, •OH is involved in an electrophilic addition of hydroxyl groups to unsaturated or unpaired groups through hydrogen atom abstraction. Additionally, it facilitates the conversion of oxygen moieties to higher oxidation states. Consequently, these oxidized

compounds are mineralized to CO_2 and H_2O.

Based on the identified products, possible pathways of chloroacetanilide herbicides by the magnetite-driven Bio-Fenton reactions are proposed in Fig. 7. The initial reactions could be induced by •OH from the Bio-Fenton reaction, which can act as both an electrophile and a nucleophile. Therefore, the herbicides may undergo oxidation through non-specific reactions involving dealkylation, dechlorination, demethoxylation, demethylation, deprotonation, and hydroxylation via hydrogen atom abstraction.

Firstly, ACC may undergo *C*-dealkylation on the side of alkyl groups, producing **(B)**. The product **(B)** could be further oxidized to **(A)** or **(D)** through *N*-dealkylation and dechlorination (Fig. 7, Top left). Meanwhile, ACC may be transformed to **(C)** through dechlorination and hydroxylation. Secondly, ALC could be oxidized to **(A)** through *C*-demethoxylation in its alkyl group, followed by dechlorination and hydroxylation with producing (B) and (C) (Fig. 7, Bottom left). These two products may be converted to (D) through *C*-demethylation and *N*-dealkylation, respectively. Thirdly, MTC may initially undergo various reactions such as *C*-demethoxylation, dealkylation, dechlorination, and hydroxylation on several chemical bonds of MTC, producing (A), (B), (C), (D), and (E) (Fig. 7, Top right). These products could be further converted to the product (F), (G), and (H) via deprotonation, dealkylation, and hydroxylation, respectively.

From these results, it found that •OH exerts random attacks on the compounds, leading to cleavage and modification at alkyl groups linked to the benzene rings of the herbicides through •OH addition. However, further oxidation was not detected in the current Bio-Fenton reaction, which rationally deduces to produce small carboxylic acids and ring-opened products (Yang et al., 2022). This lack of additional oxidation could be attributed to the insufficient amounts of H_2O_2 generated by strain C1. In addition, considering extremely short half-life (10^{-9} s) of •OH decomposing into H_2O and O_2 in an aqueous solution (Sies, 1993), the bacterial culture solution containing bacterial debris and iron mineral sludge may hamper free diffusion of •OH into the medium, resulting in lowing degradation of the target compounds.

Despite these limitations, the current Bio-Fenton reaction has remarkable advantages in terms of fairly efficient and non-selective oxidative degradation capacity with in-situ bacterial supply of H_2O_2 in the presence of magnetite under the circumneutral pH conditions. However, further research is necessary to confirm the efficacy of the current bacterial based Bio-Fenton reaction in diverse environmental media including soil, waste water, etc. In addition, further physiological and molecular biological studies for bacterial production of H_2O_2 should be followed.

3.8. Environmental implications

In the present study, it should be emphasized that the majority of products resulting from the Bio-Fenton degradation of chloroacetanilide herbicides were dechlorinated. It is widely recognized that the dechlorination of chloroacetanilide compounds helps reduce chemical toxicity and enhances biodegradability in aqueous solutions. Furthermore, magnetite, which is an abundant iron source in the earth's crust, helps the current Bio-Fenton reaction be easily adopted for the *in-situ* environmental cleanup system under circumneutral pH conditions. More importantly, the isolation of *Desemzia* sp. strain C1 having an excellent H_2O_2-producing capability could facilitate the practical application of the Bio-Fenton reaction in the actual environmental conditions. Three chloroacetanilide herbicides were selected as representative environmental pollutants; therefore, there is a potential to apply the current Bio-Fenton reaction system in the non-specific oxidative degradation of various organic compounds including various polymers of waste lignin and plastics.

4. Conclusions

In the present study, a H_2O_2-producing bacterium, *Desemzia* sp. strain C1 was isolated from oil-contaminated soil. The resting cells of strain C1 produced 1.8–2.0 mM of H_2O_2 in the presence of lactate, which was provided to the Bio-Fenton reaction. The reaction was carried out to degrade chloroacetanilide herbicides in the presence of magnetite ($Fe(II)Fe(III)_2O_4$) at pH 6.8. The optimal conditions for the reaction were 10 mM of lactate, 0.5% (w/v) of magnetite, and resting-cells ($O.D._{600}$ = 1) of strain C1. Approximately, 40–50% of the herbicides were degraded, resulting in the production of oxidized intermediates through non-specific reactions of •OH. These results could shed light on the development of the Bio-Fenton reaction, capable at a circumneutral pH conditions.

CRediT authorship contribution statement

Yongseok Ko: Writing – original draft, Methodology, Investigation,

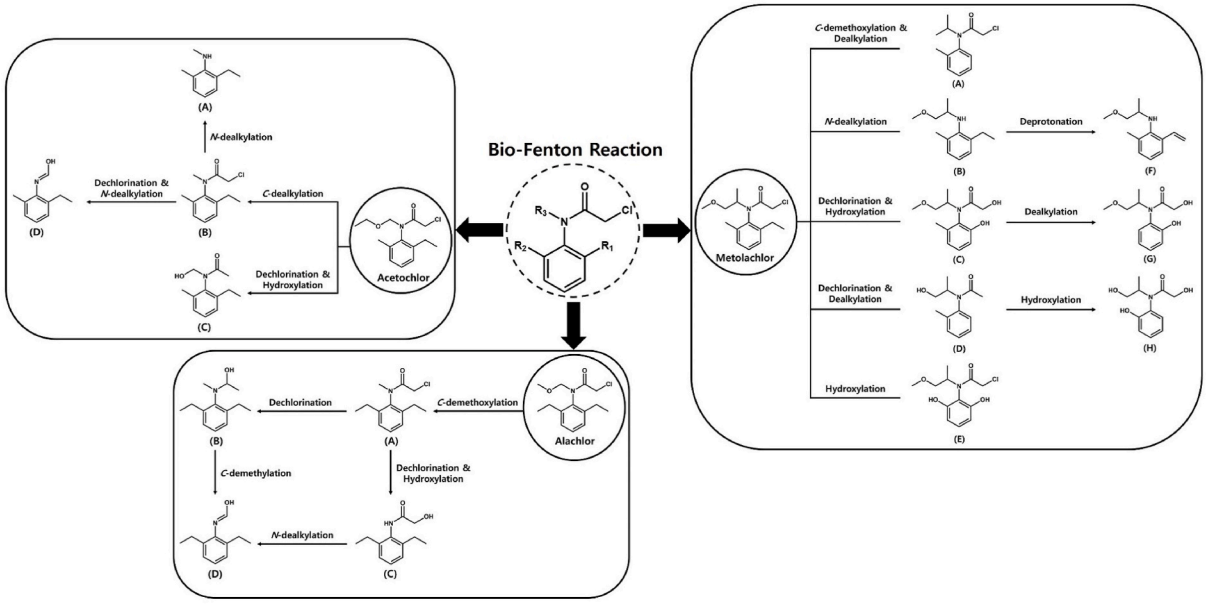

Fig. 7. Proposed pathway for the Bio-Fenton degradation of acetochlor, alachlor, and metolachlor by *Desemzia*. sp. strain C1.

Data curation. **Sunil Ghatge:** Methodology, Formal analysis. **Hor-Gil Hur:** Writing – review & editing, Writing – original draft, Supervision, Funding acquisition, Formal analysis. **Youri Yang:** Writing – review & editing, Writing – original draft, Supervision, Methodology, Investigation, Formal analysis, Conceptualization.

Declaration of competing interest

The authors declare that they have no known competing financial interests or personal relationships that could have appeared to influence the work reported in this paper.

Data availability

No data was used for the research described in the article.

Acknowledgments

This study was supported by the National Institute of Agricultural Science, Rural Development Administration, Republic of Korea (PJ0162642022) and National Research Foundation of Korea (2023R1A2C1005059). GC-MS analysis was carried out in GCRF (GIST Central Research Facilities), GIST, Gwangju, Republic of Korea. We appreciate Dr. Ji-Hoon Lee from Jeonbuk National University, Jeonju, South Korea, for helpful discussion on formation of iron mineral sludge in environments.

Appendix A. Supplementary data

Supplementary data to this article can be found online at https://doi.org/10.1016/j.chemosphere.2024.141912.

References

An, S., Yoon, Y., Ahn, J.-H., Kim, D., Weon, H.-Y., Kim, Y.-E., Hur, H.-G., Yang, Y., 2023. Oxidative degradation of bisphenol A by Bio-Fenton reaction equipped with glucose oxidase and ferric citrate: degradation kinetics and pathway. J. Environ. Chem. Eng. 11, 109349 https://doi.org/10.1016/j.jece.2023.109349.

Atwood, D., Paisley-Jones, C., 2017. Pesticides industry sales and usage 2008-2012 market estimates. Biological and Economic Analysis Division, Office of Pesticide Programs. U.S. Environmental Protection Agency (EPA), Washington, D.C.

Barnard, J.P., Stinson, M.W., 1999. Influence of environmental conditions on hydrogen peroxide formation by Streptococcus gordonii. Infect. Immun. 67, 6558–6564. https://doi.org/10.1128/iai.67.12.6558-6564.1999.

Bataineh, H., Pestovsky, O., Bakac, A., 2012. pH-induced mechanistic changeover from hydroxyl radicals to iron(iv) in the Fenton reaction. Chem. Sci. 3, 1594–1599. https://doi.org/10.1039/C2SC20099F.

Burrell, M.R., Just, V.J., Bowater, L., Fairhurst, S.A., Requena, L., Lawson, D.M., Bornemann, S., 2007. Oxalate decarboxylase and oxalate oxidase activities can be interchanged with a specificity switch of up to 282 000 by mutating an active site lid. Biochemistry 46, 12327–12336. https://doi.org/10.1021/bi700947s.

Chen, H.Y., 2019. Why the reactive oxygen species of the Fenton reaction switches from oxoiron(IV) species to hydroxyl radical in phosphate buffer solutions? A computational rationale. ACS Omega 4, 14105–14113. https://doi.org/10.1021/acsomega.9b02023.

Chen, F., Tang, D., Wang, Y., Li, T., Ma, J., 2020. Integration of homogeneous and heterogeneous advanced oxidaton processes: confined iron dancing with cyclodextrin polymer. Chemosphere 250, 126226. https://doi.org/10.1016/j.chemosphere.2020.126226.

Condon, S., 1987. Responses of lactic acid bacteria to oxygen. FEMS Microbiol. Rev. 3, 269–280. https://doi.org/10.1111/j.1574-6968.1987.tb02465.x.

Doriguetto, A.C., Fernandes, N.G., Persiano, A.I.C., Filho, E.N., Grenèche, J.M., Fabris, J. D., 2003. Characterization of a natural magnetite. Phys. Chem. Miner. 30, 249–255. https://doi.org/10.1007/s00269-003-0310-x.

Friedman, C.L., Lemley, A.T., Hay, A., 2006. Degradation of chloroacetanilide herbicides by anodic Fenton treatment. J. Agric. Food Chem. 54, 2640–2651. https://doi.org/10.1021/jf0523317.

Ghatge, S., Yang, Y., Ko, Y., Yoon, Y., Ahn, J.-H., Kim, J.J., Hur, H.-G., 2022. Degradation of sulfonated polyethylene by a bio-photo-fenton approach using glucose oxidase immobilized on titanium dioxide. J. Hazard Mater. 423, 127067 https://doi.org/10.1016/j.jhazmat.2021.127067.

Halliwell, B., Gutteridge, J.M.C., 1981. Formation of a thiobarbituric-acid-reactive substance from deoxyribose in the presence of iron salts: the role of superoxide and hydroxyl radicals. FEBS Lett. 128, 347–352. https://doi.org/10.1016/0014-5793(81)80114-7.

He, J., Yang, X., Men, B., Wang, D., 2016. Interfacial mechanisms of heterogeneous Fenton reactions catalyzed by iron-based materials: a review. J. Environ. Sci. 39, 97–109. https://doi.org/10.1016/j.jes.2015.12.003.

Hem, J.D., Cropper, W.H., 1962. Chemistry of Iron in Natural Water, Geological Survey Water-Supply Paper. Survey of ferrous-ferric chemical equilibria and redox potentials, Washington.

Henschler, D., 1994. Toxicity of chlorinated organic compounds: effects of the introduction of chlorine in organic molecules. Angew. Chem. Int. Ed. Engl. 33, 1920–1935. https://doi.org/10.1002/anie.199419201.

Hertzberger, R., Arents, J., Dekker, H.L., Pridmore, R.D., Gysler, C., Kleerebezem, M., de Mattos, M.J., 2014. H_2O_2 production in species of the Lactobacillus acidophilus group: a central role for a novel NADH-dependent flavin reductase. Appl. Environ. Microbiol. 80, 2229–2239. https://doi.org/10.1128/AEM.04272-13.

Hug, S.J., Leupin, O., 2003. Iron-catalyzed oxidation of arsenic(III) by oxygen and by hydrogen peroxide: pH-Dependent formation of oxidants in the Fenton reaction. Environ. Sci. Technol. 37, 2734–2742. https://doi.org/10.1021/es026208x.

Johnson, M., Zaretskaya, I., Raytselis, Y., Merezhuk, Y., McGinnis, S., Madden, T.L., 2008. NCBI blast: a better web interface. Nucleic Acids Res. 36, W5–W9. https://doi.org/10.1093/nar/gkn201.

Kappler, A., Newman, D.K., 2004. Formation of Fe(III)-minerals by Fe(II)-oxidizing photoautotrophic bacteria. Geochim. Cosmochim. 68, 1217–1226. https://doi.org/10.1016/j.gca.2003.09.006.

Kappler, A., Straub, K.L., 2005. Geomicrobiological cycling of iron. Rev. Mineral. Geochem. 59, 85–108. https://doi.org/10.2138/rmg.2005.59.5.

Kimura, M., 1980. A simple method for estimating evolutionary rates of base substitutions through comparative studies of nucleotide sequences. J. Mol. Evol. 16, 111–120. https://doi.org/10.1007/BF01731581.

Kleppe, K., 1966. The effect of hydrogen peroxide on glucose oxidase from Aspergillus Niger. Biochemistry 5, 139–143. https://doi.org/10.1021/bi00865a018.

Ko, Y., Yang, Y., Ghatge, S., Kim, S., Hur, H.-G., 2022. Draft genome sequence of Desemzia sp. Strain C1, producing hydrogen peroxide, isolated from oil-contaminated soil. Microbiol. Resource. Announc. 11 https://doi.org/10.1128/mra.00053-22.

Korpe, S.A., Landge, V., Hakke, V.S., Rao, P.V., Sonawane, S.H., Sonawane, S.S., 2022. Chapter 14 - advanced oxidation processes for tannery industry wastewater treatment. In: Mungray, A., Mungray, A., Sonawane, S., Sonawane, S. (Eds.), Novel Approaches towards Wastewater Treatment and Resource Recovery Technologies. Elsevier. https://doi.org/10.1016/B978-0-323-90627-2.00002-2.

Krueger, M.C., Hofmann, U., Moeder, M., Schlosser, D., 2015. Potential of wood-rotting fungi to attack polystyrene sulfonate and its depolymerisation by Gloeophyllum trabeum via hydroquinone-driven Fenton chemistry. PLoS One 10, e0131773. https://doi.org/10.1371/journal.pone.0131773.

Larkin, M.A., Blackshields, G., Brown, N.P., Chenna, R., McGettigan, P.A., McWilliam, H., Valentin, F., Wallace, I.M., Wilm, A., Lopez, R., Thompson, J.D., Gibson, T.J., Higgins, D.G., 2007. Clustal W and clustal X version 2.0. Bioinformatics 23, 2947–2948.

Lee, J.H., Roh, Y., Hur, H.G., 2008. Microbial production and characterization of superparamagnetic magnetite nanoparticles by Shewanella sp. HN-41. J. Microbiol. Biotechnol. 18, 1572–1577.

Lerro, C.C., Andreotti, G., Koutros, S., Lee, W.J., Hofmann, J.N., Sandler, D.P., Parks, C. G., Blair, A., Lubin, J.H., Beane Freeman, L.E., 2018. Alachlor use and cancer incidence in the agricultural health study: an updated analysis. J. Natl. Cancer. Inst. 110, 950–958. https://doi.org/10.1093/jnci/djy005.

Li, X., Huang, Y., Li, C., Shen, J., Deng, Y., 2015. Degradation of pCNB by Fenton like process using α-FeOOH. Chem. Eng. J. 260, 28–36. https://doi.org/10.1016/j.cej.2014.08.042.

Lian, L., Yao, B., Hou, S., Fang, J., Yan, S., Song, W., 2017. Kinetic study of hydroxyl and sulfate radical-mediated oxidation of pharmaceuticals in wastewater effluents. Environ. Sci. Technol. 51, 2954–2962. https://doi.org/10.1021/acs.est.6b05536.

Munoz, M., de Pedro, Z.M., Casas, J.A., Rodriguez, J.J., 2015. Preparation of magnetite-based catalysts and their application in heterogeneous Fenton oxidation - a review. Appl. Catal. B Environ. 176–177, 249–265. https://doi.org/10.1093/bioinformatics/btm404.

Panda, N., Sahoo, H., Mohapatra, S., 2011. Decolourization of methyl orange using Fenton-like mesoporous Fe_2O_3-SiO_2 composite. J. Hazard Mater. 185, 359–365. https://doi.org/10.1016/j.jhazmat.2010.09.042.

Park, S., Lee, J.-H., Shin, T.J., Hur, H.-G., Kim, M.G., 2018. Adsorption and incorporation of arsenic to biogenic lepidocrocite formed in the presence of ferrous iron during denitrification by Paracoccus denitrificans. Environ. Sci. Technol. 52, 9983–9991. https://doi.org/10.1021/acs.est.8b02101.

Patel, S.K., Patel, S.G., Patel, G.V., 2020. Degradation of reactive dye in aqueous solution by Fenton, photo-Fenton process and combination process with activated charcoal and TiO_2. Proc. Natl. Acad. Sci. India. Sect. A Phys. Sci. 90, 579–591. https://doi.org/10.1007/s40010-019-00618-3.

Piepenbrock, A., Dippon, U., Porsch, K., Appel, E., Kappler, A., 2011. Dependence of microbial magnetite formation on humic substance and ferrihydrite concentrations. Geochim. Cosmochim. Acta. 75, 6844–6858. https://doi.org/10.1016/j.gca.2011.09.007.

Qin, Y., Song, F., Ai, Z., Zhang, P., Zhang, L., 2015. Protocatechuic acid promoted alachlor degradation in Fe(III)/H_2O_2 Fenton system. Environ. Sci. Technol. 49, 7948–7956. https://doi.org/10.1021/es506110w.

Qin, Q., Liu, Y., Li, X., Sun, T., Xu, Y., 2018. Enhanced heterogeneous Fenton-like degradation of methylene blue by reduced $CuFe_2O_4$. RSC Adv. 8, 1071–1077. https://doi.org/10.1039/C7RA12488K.

Saito, M., Seki, M., Iida, K., Nakayama, H., Yoshida, S., 2007. A novel agar medium to detect hydrogen peroxide-producing bacteria based on the prussian blue-forming

reaction. Microbiol. Immunol. 51, 889–892. https://doi.org/10.1111/j.1348-0421.2007.tb03971.x.
Saitou, N., Nei, M., 1987. The neighbor-joining method: a new method for reconstructing phylogenetic trees. Mol. Biol. Evol. 4, 406–425. https://doi.org/10.1093/oxfordjournals.molbev.a040454.
Schwertmann, U., Cornell, R.M., 2000. In Iron Oxides in the Laboratory: Preparation and Characterization, Chapter 1- the Iron Oxides. Wiley-VCH, pp. 5–18.
Sies, H., 1993. Strategies of antioxidant defense. Eur. J. Biochem. 215, 213–219. https://doi.org/10.1111/j.1432-1033.1993.tb18025.x.
Solís-López, M., Durán-Moreno, A., Rigas, F., Morales, A.A., Navarrete, M., Ramírez-Zamora, R.M., 2014. Chapter 9 - assessment of copper slag as a sustainable Fenton-type photocatalyst for water disinfection. In: Ahuja, S. (Ed.), Water Reclamation and Sustainability. Elsevier, pp. 199–227. https://doi.org/10.1016/B978-0-12-411645-0.00009-2.
Stackebrandt, E., 2015. Desemzia. In: Bergey's Manual of Systematics of Archaea and Bacteria. John Wiley & Sons, Inc., pp. 1–9
Stanier, R.Y., Palleroni, N.J., Doudoroff, M., 1966. The aerobic Pseudomonads a taxonomic study. Microbiology 43, 159–271. https://doi.org/10.1099/00221287-43-2-159.
Steinhaus, E.A., 1941. A study of the bacteria associated with thirty species of insects. J. Bacteriol. 42, 757–790. https://doi.org/10.1128/IAI.67.12.6558-6564.1999.
Taniai, H., Iida, K., Seki, M., Saito, M., Shiota, S., Nakayama, H., Yoshida, S., 2008. Concerted action of lactate oxidase and pyruvate oxidase in aerobic growth of Streptococcus pneumoniae: role of lactate as an energy source. J. Bacteriol. 190, 3572–3579. https://doi.org/10.1128/JB.01882-07.
Tsyganok, A.I., Otsuka, K., 1999. Selective dechlorination of chlorinated phenoxy herbicides in aqueous medium by electrocatalytic reduction over palladium-loaded carbon felt. Appl. Catal. B Environ. 22, 15–26. https://doi.org/10.1016/S0926-3373(99)00028-4.
U.S. Environmental Protection Agency (EPA), 1998. Office of Pesticide Programs. EPA Registration eligibiliity decision (RED) Alachlor (EPA-738-R-98-020)., Washington, D.C.
Xu, L., Wang, J., 2012. Fenton-like degradation of 2,4-dichlorophenol using Fe_3O_4 magnetic nanoparticles. Appl. Catal. B Environ. 123–124, 117–126. https://doi.org/10.1016/j.apcatb.2012.04.028.
Yang, Y., Ghatge, S., Ko, Y., Yoon, Y., Ahn, J.-H., Kim, J.J., Hur, H.-G., 2022. Non-specific degradation of chloroacetanilide herbicides by glucose oxidase supported Bio-Fenton reaction. Chemosphere 292, 133417. https://doi.org/10.1016/j.chemosphere.2021.133417.
Zhao, L., Lin, Z.-R., Ma, X.-h., Dong, Y.-H., 2018. Catalytic activity of different iron oxides: insight from pollutant degradation and hydroxyl radical formation in heterogeneous Fenton-like systems. Chem. Eng. J. 352, 343–351. https://doi.org/10.1016/j.cej.2018.07.035.